Doping Variation of Orbitally Induced Anisotropy in the Electronic Structure of $La_{1-x}Sr_xVO_3$

J. Fujioka,[1] S. Miyasaka,[1] and Y. Tokura[1,2,3]

[1]*Department of Applied Physics, University of Tokyo, Tokyo 113-8656, Japan*
[2]*Spin Superstructure Project, ERATO, Japan Science and Technology Agency, Tsukuba, 305-8562, Japan*
[3]*Correlated Electron Research Center (CERC), National Institute of Advanced Industrial Science and Technology (AIST), Tsukuba 305-8562, Japan*

(Received 26 May 2006; published 10 November 2006)

The variation of anisotropic charge dynamics in the course of a filling-control insulator-metal transition (IMT) in $La_{1-x}Sr_xVO_3$ has been investigated by measurements of optical conductivity spectra with the focus on the role of the t_{2g}-orbital degree of freedom. The orbitally induced anisotropic feature of the Mott-gap excitation as well as of the doping-induced midinfrared excitation is suppressed with increasing x, and instead the isotropic and incoherent dynamics of the doped hole dominates over the low-energy excitation near and above the IMT point.

DOI: 10.1103/PhysRevLett.97.196401 PACS numbers: 71.30.+h, 72.15.−v, 75.30.Et, 78.20.−e

The orbital degree of freedom in the strongly correlated electron system plays an essential role in producing versatile phenomena via its coupling with charge, spin, and lattice dynamics [1,2]. One such example is the colossal magnetoresistance effect in the perovskite manganites where the dramatic reconstruction of the electronic structure can be observed in the vicinity of the insulator-metal transition (IMT) accompanying the orbital order-disorder phenomenon [3]. In the manganites, the orbital ordering transition and the concomitant change of the charge transport property are strongly tied with the lattice degree of freedom through the cooperative Jahn-Teller coupling of the conduction e_g electron. In the t_{2g} orbital system, by contrast, the energy scale of the Jahn-Teller effect is comparable to that of the intersite spin-orbital exchange interaction as well as to that of the intra-atomic spin-orbit one [4,5]. This results in the large spin-orbital quantum fluctulation, responsible for anomalous spin dynamics [6,7] and orbital excitations [8,9]. The quantum-mechanical aspect of the spin-orbital coupling may be also visible in the charge dynamics as well as the spin dynamics. One representative example of the t_{2g}-orbital systems is $LaVO_3$, also known as the prototypical Mott-Hubbard type insulator. $LaVO_3$ has a pseudocubic perovskite structure and the electron configuration of the nominally trivalent vanadium ion is $3d^2$ (t_{2g}^2) with $S = 1$. The spin moment is approximately $1.3\mu_B$ and much smaller than the free-ion moment $2\mu_B$ for $S = 1$, reflecting large spin-orbital quantum fluctuation [4,7,10]. Since the orthorhombic lattice distortion lifts the degeneracy of t_{2g} levels, one electron always occupies the d_{xy} orbital but another one does either the d_{yz} or d_{zx} orbital, retaining the orbital degree of freedom. With lowering temperature (T), the C-type spin ordering (SO) appears at $T_{SO} = 143$ K, where spins align ferromagnetically along the c axis and antiferromagnetically in the ab plane [11,12]. Subsequently, the G-type orbital ordering (OO) appears at $T_{OO} = 141$ K, where occupied d_{zx} and d_{yz} orbitals are staggered in all (x, y, z) directions. Recent studies have revealed the highly one-dimensional (1D) nature of the orbital exchange interaction along the c axis, which is realized in the C-type spin-ordered and G-type orbital-ordered phase due to the interference type cancellation of the ab-plane interaction [5,8,13]. In contrast to a naive view of this nearly cubic lattice systems, the spin-orbital ordering induces the huge anisotropy of the Mott-gap transition spectrum [14], the variation of which with doping is the subject of the present study.

As shown in the inset of Fig. 1, the nominal hole doping (x) in the form of $La_{1-x}Sr_xVO_3$ induces the filling-control IMT at the critical doping level $x_c = 0.176$, accompanying the melting of the G-type OO [15]. We reproduce in Fig. 1 the T dependence of the resistivity for $La_{1-x}Sr_xVO_3$. For $x < x_c$, a clear kink is observed corresponding to the onset

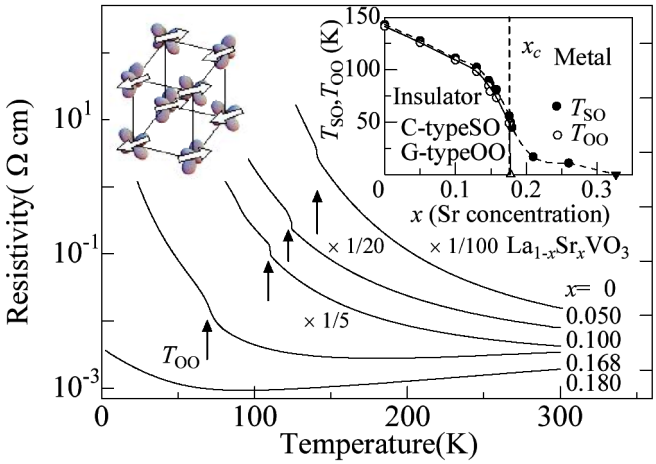

FIG. 1 (color online). Temperature dependence of resistivity for single crystals of $La_{1-x}Sr_xVO_3$ ($x = 0$, 0.050, 0.100, 0.168, and 0.180). Sets show the electronic phase diagram plotted against the doping level x, and the orbital and spin ordering pattern in $LaVO_3$.

of the G-type OO. For $x = 0$ and $x = 0.050$, the resistivity along the c axis was found to be nearly identical to that in the ab plane within an experimental error, showing essentially no anisotropy of charge dynamics in the C-type spin-ordered and G-type orbital-ordered state in the dc limit. This is perhaps because of the nearly full-gap nature in the low-doped region, and the active role of the orbital ordering should be explored in the finite-frequency (optical) region even in the hole-doped crystals. Motivated by this and also by the filling-control IMT feature concomitant with the orbital disordering [15], we have investigated here the doping variation of the anisotropic electronic structure in single crystals of $La_{1-x}Sr_xVO_3$ by measurements of the optical conductivity spectra [$\sigma(\omega)$].

In Figs. 2(a) and 2(b), we show the $\sigma(\omega)$ spectra for $x = 0$, 0.050, 0.100, 0.168, and 0.180 at 10 K with the light polarizations parallel ($E \parallel c$) and perpendicular ($E \perp c$), respectively, to the c axis. All the single crystals of $La_{1-x}Sr_xVO_3$ investigated here were grown by a floating-zone method, as detailed in Ref. [15]. The $\sigma(\omega)$ spectra were obtained by a Kramers-Kronig analysis of polarized reflectivity spectra between 10 meV and 40 eV, as described in [14]. For $x = 0$, the $E \parallel c$ spectra ($\sigma_{\parallel}(\omega)$) shows the prominent peak structure originating from the Mott-gap excitation around 2 eV. For the lightly doped compound with $x = 0.050$, the spectral weight of the Mott-gap excitation decreases as compared with that for $x = 0$, while a midinfrared (mid-IR) peak, which results from the incoherent motion of the doped hole, is observed in the midgap (1 eV) region [1,16]. With further increasing x, the mid-IR peak gradually increases in magnitude with shifting toward lower energy. Such a spectral weight transfer from the Mott-gap excitation to the mid-IR peak as leading to the charge-gap closing is consistent with the previous report on the unpolarized spectra on the polycrystals [16] and commonly observed for other filling-control IMT systems [1]. In the spectra for $E \perp c$ [$\sigma_{\perp}(\omega)$], on the other hand, the spectral weight around 2 eV is small and remains nearly independent of x, whereas that of the mid-IR peak increases with doping, similar to that for the $\sigma_{\parallel}(\omega)$ spectra.

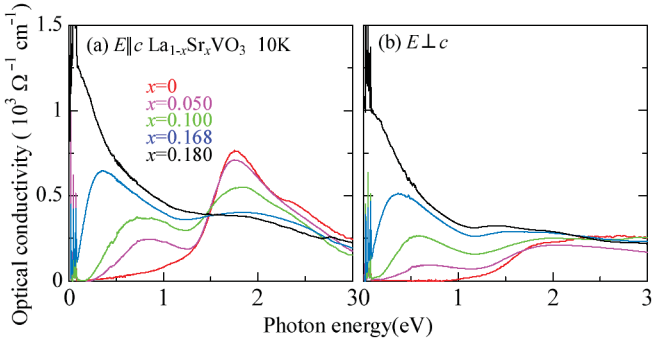

FIG. 2 (color). (a) The optical conductivity spectra of $La_{1-x}Sr_xVO_3$ with various doping levels ($x = 0$, 0.050, 0.100, 0.168, and 0.180) at 10 K for $E \parallel c$ and (b) those for $E \parallel c$.

The polarization dependence of the $\sigma(\omega)$ spectra at the respective doping levels at 10 K is shown in Figs. 3(a)–3(c). As clearly seen in Fig. 3(a), the spectral weight around 2 eV for the $\sigma_{\parallel}(\omega)$ spectrum for $x = 0.050$ is much larger than that for the $\sigma_{\perp}(\omega)$ one, due to the quasi-1D orbital exchange interaction along the c axis in the C-type spin-ordered and G-type orbital-ordered phase, as well as for $x = 0$ [5]. The spectral weight around 1 eV for the $\sigma_{\parallel}(\omega)$ spectrum is also much larger than that for the $\sigma_{\perp}(\omega)$ one, implying the anisotropic dynamics of the doped hole. As x increases, the anisotropy of the $\sigma(\omega)$ spectrum around 1 eV is gradually suppressed as well as that for the Mott-gap excitation and finally almost disappears for $x = 0.168$ or upon the IMT.

To quantify the respective spectral weights of the Mott-gap excitation and the incoherent motion of the doped hole, both $\sigma_{\parallel}(\omega)$ and $\sigma_{\perp}(\omega)$ spectra are fitted with the Lorentz oscillators, expressed by the following formula,

$$\sigma(\omega) = \frac{\sigma(0)}{1 + \omega^2\tau^2} + \sum_{j=m,\mathrm{mg1},\mathrm{mg2},\mathrm{ct}} \frac{S_j\gamma_j\omega^2\omega_j^2}{(\omega^2 - \omega_j^2)^2 + \gamma_j^2\omega^2}, \quad (1)$$

where the τ, S_i, γ_j, and ω_j represent the scattering time of the coherent part, the oscillator strength, the damping

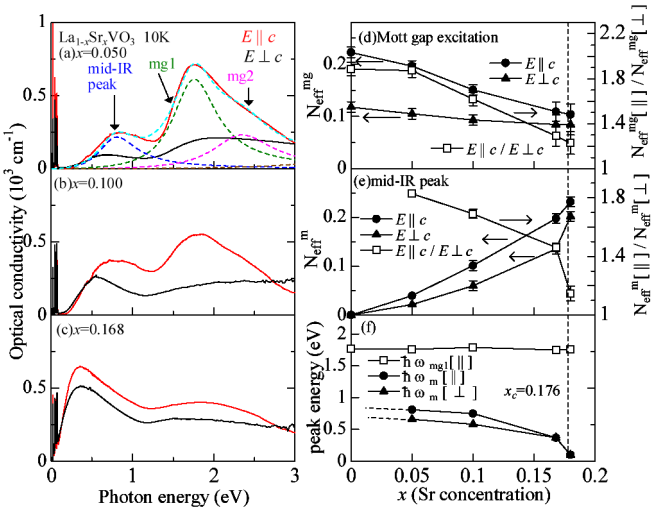

FIG. 3 (color online). (a)–(c) The polarization dependence of the optical conductivity spectra of $La_{1-x}Sr_xVO_3$ ($x = 0.050$, 0.100, and 0.168) at 10 K, respectively. (d) The effective number of electrons (spectral weight) of the Mott-gap excitation ($N_{\mathrm{eff}}^{\mathrm{mg}}$) for $E \parallel c$ and $E \perp c$ spectra plotted against the doping level x. The x dependence of the ratio $N_{\mathrm{eff}}^{\mathrm{mg}}[\parallel]/N_{\mathrm{eff}}^{\mathrm{mg}}[\perp]$ is also shown. The vertical dashed line represents the critical doping level (x_c) for the insulator-metal transition. (e) The effective number of electrons (spectral weight) of the mid-IR component (N_{eff}^{m}) for $E \parallel c$ and $E \perp c$ spectra plotted against the doping level x. The x dependence of the ratio $N_{\mathrm{eff}}^{m}[\parallel]/N_{\mathrm{eff}}^{m}[\perp]$ is also shown. (f) The mid-IR peak energy for $E \parallel c$ and $E \perp c$ and that of the Mott-gap excitation for $E \parallel c$ plotted against x (see text for definition).

constant (broadening parameter), and the frequency of the jth Lorentz oscillator, respectively. The first term is the Drude component which is only present for the metallic compound, $x = 0.180$. The second term is composed of the sum of the mid-IR peak ($j = m$), the two components of the Mott-gap excitation ($j =$ mg1 and mg2) and the charge transfer excitation ($j =$ ct) [14]. As assigned in [14], the lower-lying mg1 band is an allowed Mott-gap transition along the ferromagnetic chain ($\| c$) in the C-type spin-ordered state, while the higher-lying mg2 band with a different final state on the V site is only weakly allowed due to the imperfect spin-orbital polarization. The result for fitting and the respective components of the $\sigma_{\|}(\omega)$ spectrum are exemplified for $x = 0.050$ in Fig. 3(a). After the decomposition of the $\sigma(\omega)$, we calculated the effective number of electrons (N_{eff}) contributing to each (jth) component as a measure of the spectral weight by the following formula, $N_{\mathrm{eff}}^{(j)} = \frac{2m}{\pi e^2 N} \int_0^{\infty} \sigma^{(j)}(\omega) d\omega$. Here m and N are the bare electron mass and the number of V sites per unit volume, respectively [17].

Figure 3(d) shows the N_{eff} of the Mott-gap excitation in $\sigma_{\|}(\omega)$ and $\sigma_{\perp}(\omega)$ spectra at 10 K, $N_{\mathrm{eff}}^{\mathrm{mg}}[\|]$ and $N_{\mathrm{eff}}^{\mathrm{mg}}[\perp]$, respectively, as a function of x. Here, $N_{\mathrm{eff}}^{\mathrm{mg}}$ is defined as the sum of the two components (mg1 and mg2) of the Mott-gap excitation. We also plot the ratio $N_{\mathrm{eff}}^{\mathrm{mg}}[\|]/N_{\mathrm{eff}}^{\mathrm{mg}}[\perp]$ as a measure of the anisotropy in the Mott-gap excitation. For $x = 0$, $N_{\mathrm{eff}}^{\mathrm{mg}}[\|]/N_{\mathrm{eff}}^{\mathrm{mg}}[\perp] \sim 1.8$, indicating the large anisotropic feature of the Mott-gap excitation due to the quasi-1D orbital exchange interaction [5]. With increasing x, $N_{\mathrm{eff}}^{\mathrm{mg}}[\|]$ decreases more rapidly than $N_{\mathrm{eff}}^{\mathrm{mg}}[\perp]$ and the ratio $N_{\mathrm{eff}}^{\mathrm{mg}}[\|]/N_{\mathrm{eff}}^{\mathrm{mg}}[\perp]$ decreases monotonously toward unity (isotropic limit). This implies that the doped holes reduce the spin and orbital correlation and the quasi-1D orbital exchange interaction disappears in accord with the melting of the G-type OO. A similar behavior is observed in the mid-IR component. In Fig. 3(e), we plot the x dependence of the spectral weight of the mid-IR component in $\sigma_{\|}(\omega)$ and $\sigma_{\perp}(\omega)$ spectra at 10 K, $N_{\mathrm{eff}}^{m}[\|]$ and $N_{\mathrm{eff}}^{m}[\perp]$, respectively. With increasing x, both $N_{\mathrm{eff}}^{m}[\|]$ and $N_{\mathrm{eff}}^{m}[\perp]$ increase monotonously and exceed that of the Mott-gap excitation in the vicinity of the IMT. Concomitantly, the ratio $N_{\mathrm{eff}}^{m}[\|]/N_{\mathrm{eff}}^{m}[\perp]$ decreases and the spectral weight of the mid-IR component becomes less polarization dependent. This indicates that with the increase of hole concentration the isotropic charge dynamics originating from the coherent and/or incoherent hole motion dominates over the low-energy excitation.

In Fig. 3(f), we also display the x dependence of the mid-IR peak energy $\hbar\omega_m$ for the $\sigma_{\|}(\omega)$ spectrum ($\hbar\omega_m[\|]$) and that for the $\sigma_{\perp}(\omega)$ one ($\hbar\omega_m[\perp]$) together with that for the Mott-gap excitation in $\sigma_{\|}(\omega)$ ($\hbar\omega_{\mathrm{mg1}}[\|]$). According to the theoretical calculation on the hole dynamics dressed with the t_{2g} orbital excitations (orbitons) [18], $\hbar\omega_m[\|]$ is anticipated to be $\sim$10 meV, which is much less than the observed result, $\hbar\omega_m[\|] \sim 0.7$ eV. This implies that other factors than the orbiton play a significant role in determining the excitation of the doped hole. One possible factor is the lattice relaxation effect around the doped hole: The doped hole would be trapped to form in the local bound state accompanying the deformation in all the spin, orbital, and lattice sectors, as observed for other doped Mott insulators [19,20]. In the lightly doped region, e.g., at $x = 0.050$ and 0.100, both $\hbar\omega_m[\|]$ and $\hbar\omega_m[\perp]$ appear to be nearly independent of x, and $N_{\mathrm{eff}}^{m}[\|]$ and $N_{\mathrm{eff}}^{m}[\perp]$ seem to be proportional to x, implying that the doped holes locally modulate the electronic state around themselves without significant interaction between them. In the close vicinity of, or beyond, the IMT critical doping ($x_c = 0.176$), the $\hbar\omega_m$ and the spectral weight of the mid-IR component become isotropic with respect to the polarization, which ensures the orbital melting feature of the IMT [15]. Furthermore, $\hbar\omega_{\mathrm{mg1}}[\|]$ is nearly independent of x, indicating the subsistence of the Mott-gap feature right up to the metallic region.

Next, we focus on the T dependence of the electronic structure. In Figs. 4(a)–4(e), we display the T dependence of the $\sigma_{\|}(\omega)$ spectra at the respective doping levels. For $x = 0$, with lowering T the spectral weight of the Mott-gap excitation is enhanced, which reflects the quasi-1D orbital exchange interaction arising from the C-type SO and the G-type OO [14]. The Mott-gap excitation are T dependent below a T (e.g., 293 K) far above T_{SO} and T_{OO} due to the subsistence of the spin and orbital fluctuation. For the doped compounds, the Mott-gap excitation shows similar T dependence. However, the magnitude of the T dependence appears to be gradually suppressed with increasing x

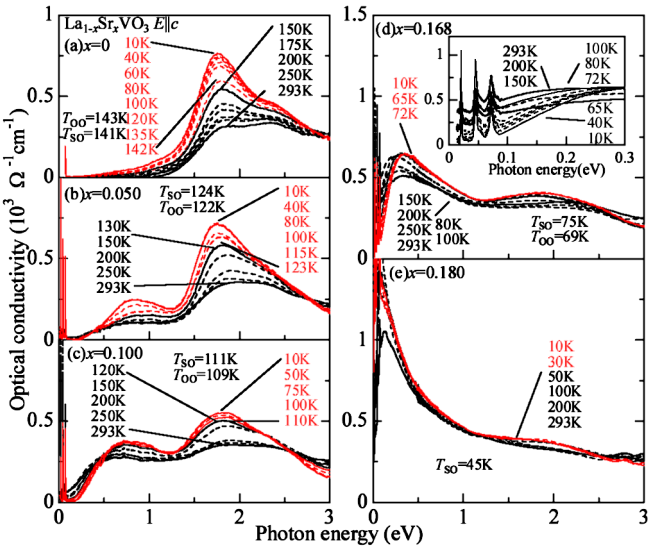

FIG. 4 (color online). (a)–(e) Temperature dependence of the optical conductivity spectra of $La_{1-x}Sr_xVO_3$ ($x = 0$, 0.050, 0.100, 0.168, and 0.180) for $E \| c$, respectively. The inset shows the magnified view of the optical conductivity spectra below 0.3 eV of $La_{1-x}Sr_xVO_3$ with $x = 0.168$ for $E \| c$.

perhaps due to the reduction of the spin and orbital correlation. The T dependence of the mid-IR peak also shows an anisotropic behavior with respect to the polarization. At the low-doping level, e.g., $x = 0.050$, the spectral weight of the mid-IR peak for $\sigma_{\|}(\omega)$ spectra increases with lowering T, especially around T_{SO} and T_{OO}, similarly to that of the higher-lying Mott-gap excitation. Such a behavior is contrasted by that for $\sigma_{\perp}(\omega)$ spectra which show the minimal T dependence (not shown). Note that with lowering T, the spectral weight below 0.5 eV decreases, leading to the charge-gap opening. With increasing x, the T dependence of the mid-IR peak is gradually suppressed, but the charge-gap formation remains to be clearly observed in the C-type spin-orbital-ordered and the G-type orbital-ordered phase. On the other hand, in the vicinity of the IMT, e.g., at $x = 0.168$, with lowering T from 293 to 150 K, the spectral weight below 0.3 eV once increases, and then decreases below 150 K with the formation of the charge gap, as shown in the inset of Fig. 4(d). This is consistent with the T dependence of resistivity, which shows a metallic behavior in the high-T region above 150 K, but becomes insulating in the low-T region. Such a thermally induced crossover from the high-T metallic to the low-T insulating behavior is a generic feature in the vicinity of the Mott transition [21,22] and appears in the present case to results from the C-type SO and the G-type OO correlation.

These T dependencies of the mid-IR component may be explained in terms of the orbital-dependent hole dynamics in the course of the melting of the G-type OO. The large enhancement of the mid-IR peak for $\sigma_{\|}(\omega)$ around T_{OO} observed in the lightly doped region indicates that the onset of the C-type SO and G-type OO is responsible for the increase of the kinetic energy of the doped hole along the c axis. Since the electrons in d_{xy} orbital would not contribute to $N_{\mathrm{eff}}^{m}[\|]$, it is expected that the doped hole predominantly occupies the d_{yz} or d_{zx} orbitals, where the effective hopping of the electron is larger along the c axis than within the ab plane due to the quasi-1D orbital exchange interaction. In this picture, the evolution of the gap feature for the $\sigma_{\|}(\omega)$ in the low T region and the fact that $\hbar\omega_m[\|] > \hbar\omega_m[\perp]$ may be explained in terms of the enhancement of electron correlation or the resultant formation of a polaron [23]. Note that the mid-IR peak as well as the Mott-gap excitation shows discernible T dependence above T_{SO} and T_{OO}; the short range spin and orbital fluctuation locally modifies the kinetic energy of the doped holes. In the x region close to the IMT point, however, the T dependence of the mid-IR peak no longer shows anisotropic behavior, suggesting that the doped hole may almost equivalently occupy the d_{xy}, d_{yz}, and d_{zx} orbitals and that the anisotropy of the electron hopping almost disappears. This coincides with the orbital melting feature of the IMT [15].

In summary, we have investigated the polarization and temperature dependence of optical conductivity spectra for single-domain single crystals of $La_{1-x}Sr_xVO_3$. The optical conductivity spectrum is reconstructed over a wide energy range up to 5 eV in the course of the filling-control IMT. In the lightly doped region the doped hole predominantly occupies the d_{yz} or d_{yz} orbital and forms the bound state or polaron with large transition intensity for $E \| c$, reflecting the quasi-1D orbital exchange interaction. As the filling-control IMT point is approached, the quasi-1D orbital exchange interaction is weakened and the anisotropy of the conductivity spectrum is suppressed, while the isotropic incoherent motion of the doped hole dominates over the low-energy optical excitation. These results suggest that the doped holes tend to equivalently occupy the d_{yz}, d_{yz}, and d_{xy} orbital, leading to the orbital melting upon the IMT.

We would thank S. Ishihara for enlightening discussion. This work was supported by KAKENHI (No. 16740192, No. 17340104, No. 15104006) and TOKUTEI (No. 16076205) from JPSJ and MEXT.

[1] For a review, M. Imada, A. Fujimori, and Y. Tokura, Rev. Mod. Phys. **70**, 1039 (1998).
[2] Y. Tokura and N. Nagaosa, Science **288**, 462 (2000).
[3] For a review, see, for example, Y. Tokura, Rep. Prog. Phys. **69**, 797 (2006).
[4] G. Khaliullin, P. Horsch, and A. M. Oles, Phys. Rev. Lett. **86**, 3879 (2001).
[5] Y. Motome *et al.*, Phys. Rev. Lett. **90**, 146602 (2003).
[6] B. Keimer *et al.*, Phys. Rev. Lett. **85**, 3946 (2000).
[7] C. Ulrich *et al.*, Phys. Rev. Lett. **91**, 257202 (2003).
[8] S. Miyasaka *et al.*, Phys. Rev. Lett. **94**, 076405 (2005).
[9] S. Miyasaka *et al.*, Phys. Rev. B **73**, 224436 (2006).
[10] V. G. Zubkov, G. V. Bazuev, and G. P. Shveikin, Sov. Phys. Solid State **18**, 1165 (1976).
[11] P. Bordet *et al.*, J. Solid State Chem. **106**, 253 (1993).
[12] S. Miyasaka *et al.*, Phys. Rev. B **68**, 100406(R) (2003).
[13] G. Khaliullin, P. Horsch, and A. M. Oles, Phys. Rev. B **70**, 195103 (2004).
[14] S. Miyasaka, Y. Okimoto, and Y. Tokura, J. Phys. Soc. Jpn. **71**, 2086 (2002).
[15] S. Miyasaka, T. Okuda, and Y. Tokura, Phys. Rev. Lett. **85**, 5388 (2000).
[16] F. Inaba *et al.*, Phys. Rev. B **52**, R2221 (1995).
[17] For $x = 0.180$, it is difficult to distinguish the mid-IR peak and the Drude part experimentally due to the merged broad-peak structure. Thus, we do not discuss separately these two components, and defined ''mid-IR component'' as the sum of them for this compound.
[18] S. Ishihara, Phys. Rev. Lett. **94**, 156408 (2005).
[19] C. Bernhard *et al.*, Phys. Rev. Lett. **93**, 167003 (2004).
[20] J. Geck *et al.*, Phys. Rev. Lett. **95**, 236401 (2005).
[21] M. J. Rozenberg *et al.*, Phys. Rev. Lett. **75**, 105 (1995).
[22] Y. Tokura *et al.*, Phys. Rev. B **58**, R1699 (1998).
[23] R. Kilian and G. Khaliullin, Phys. Rev. B **60**, 13 458 (1999).